Relationship between Liquid Nanoscale Structure in Solvents and the Strength of the Hofmeister Effect in Extraction Experiments

Journal:	*Physical Chemistry Chemical Physics*
Manuscript ID	CP-ART-11-2020-005973.R2
Article Type:	Paper
Date Submitted by the Author:	24-Feb-2021
Complete List of Authors:	Kobrak, Mark; Brooklyn College of the City University of New York, Department of Chemistry; Graduate Center of the City University of New York, Department of Chemistry Nykypanchuk, Dmytro; Brookhaven National Laboratory , Center for Functional Nanomaterials Janssen, Camiel; Universidad Nacional Autonoma de Mexico, Ingeniería Química, Facultad de Química

Relationship between Liquid Nanoscale Structure in Solvents and the Strength of the Hofmeister Effect in Extraction Experiments

Mark N. Kobrak[a,b], Dmytro Nykypanchuk[c], and Camiel H. C. Janssen[d]*

[a] Prof. Mark N. Kobrak, Department of Chemistry, Brooklyn College of the City University of New York, 2900 Bedford Ave., Brooklyn, NY 11210

[b] Prof. M.N. Kobrak, Department of Chemistry, Graduate Center of the City University of New York, 365 Fifth Ave., New York, NY 10016

[c] Dr. Dmytro Nykypanchuk, Center for Functional Nanomaterials, Brookhaven National Laboratory, Upton, NY 11973

[*d] Corresponding author: Dr. C.H.C. Janssen, Departamento de Ingeniería Química, Facultad de Química, Universidad Nacional Autónoma de México, Circuito Exterior S/N, Coyoacán, Cd. Universitaria, 04510 Ciudad de México, CDMX. Email: engineerjanssen@gmail.com

Keywords: Hofmeister effect, metal extraction, nanostructures, pseudo-protic ionic liquids, SAXS.

Abstract:

In this study, we used mixtures of carboxylic acids and amines as solvents for the liquid-liquid extraction of copper salts with various anions from aqueous phase, and systematically varied the acid/amine ratio to determine its influence on extraction efficiency. The organic phases resulting from these extraction experiments were studied using small-angle X-ray scattering (SAXS), establishing a connection between the extraction process and the liquid structure. A relationship is found between the extent of extraction for the metal salt, the strength of the Hofmeister effect of the anions of the salt, and the characteristic lengthscale of the observed liquid nanoscale structure before and after extraction.

Introduction:

The past two decades have seen a renaissance in the development of novel solvent systems, including examples such as ionic liquids[1–3] and deep eutectics.[3,4] Recently mixtures of carboxylic acids and tertiary amines were studied for use in liquid-liquid biphasic extraction of copper salts.[5] This class of liquids has been of interest for their utility in the extraction of salts and acids from aqueous phase.[6–8]

Tertiary amine/carboxylic acid mixtures are known to form strong hydrogen-bonding networks at specific amine:acid mole ratios (e.g. 3 acid:1 amine).[9,10] In a 1:1 molar ratio of acid to amine, these systems are similar to protic ionic liquids,[11] and some researchers refer to these 1:1 systems as “pseudoprotic ionic liquids”.[12,13] Recently this work was extended using SAXS to directly observe the structure associated with the nanoscale liquid structure resulting from the hydrogen-bonded network at various acid/amine ratios in the water-saturated mixtures.[14] These observations, combined with data from studies of metal extraction,[5] suggest a possible relationship between the local structure of these mixtures and their behavior as solvents for the extraction of metal salts from aqueous phase. In the present study we combine extraction and SAXS experiments to characterize this link.

Mechanisms of metal ion extraction

The cations and anions of a metal salt can be extracted from the aqueous phase to the protic mixture through several mechanisms, as given in Table 1. The range of possible mechanisms is constrained by the need to maintain charge balance between the phases. While in many of the reported experiments more than one mechanism is at work, their relative importance can be inferred by comparison of the extent of extraction for the metal cation and its corresponding anion.

Mechanism	**Net Ionic Equation**
Neutral Extraction	$M^{2+}(aq) + 2X^{-}(aq) \leftrightarrow M^{2+}(org) + 2X^{-}(org)$
Cation Exchange	$M^{2+}(aq) + 2HA\,(org) \leftrightarrow M^{2+}(org) + 2H^{+}(aq) + 2A^{-}(org)$
Anion Exchange	$X^{-}(aq) + HA\,(org) \leftrightarrow X^{-}\,(org) + H^{+}(org) + A^{-}(aq)$

Table 1: Possible mechanisms for extraction from aqueous to organic phase (denoted “(org)”). Mechanisms are written assuming monovalent anions (X^{-}) and divalent metal cations (M^{2+}), though are equally applicable for divalent sulfate anions. “HA” denotes an organic acid, and “A^{-}” denotes its conjugate base. The equations presented are schematic and are not intended to imply the coordination state of the ions in either phase.

It has been observed previously that all of these processes are at work in the extraction of copper salts from aqueous phase to amine/acid mixtures, and the identity of the anion plays an important role in the mechanism and extent of extraction.[5] This dependence on the anion arises from the Hofmeister effect.

The Hofmeister effect

The Hofmeister effect has been known for over a century,[15] and has been observed in a wide range of contexts including the salting in/out of proteins,[16] chromatography,[17] and the formation of amphiphilic aggregates in aqueous phase.[18,19] A common thread in these phenomena is that ions can influence the structure and energetics of hydrophobic/hydrophilic domain interfaces, and the extent of this influence depends on the identity of the ion.

Strikingly, the relative capacities of different ions to contribute to this effect is consistent across an enormous range of phenomena. This gives rise to the Hofmeister series, in which ions are ordered based on the strength of their contribution to the Hofmeister effect. A sample series for anions is given in Figure 1; an analogous series exists for cations. Ions on the right of the series are referred to as chaotropic and those on the left are said to be kosmotropic.

One example of the Hofmeister effect is in the changes in critical micelle concentration (CMC) for amphiphiles in aqueous salt solutions. The CMC for ionic surfactants generally decreases in electrolyte solutions, with the value of the CMC decreasing further as the ions composing the electrolyte become more chaotropic.[20,21] For nonionic surfactants, the reverse is often true, with the CMC increasing with the chaotropic character of the electrolyte.[22,23] While the trends run in opposite directions, in both cases the observed variation is generally consistent with the Hofmeister series. This is only one example of the strong relationship between the Hofmeister effect and the morphology of aggregates in solution.

The relevance of the Hofmeister effect to the extraction of metal salts in protic mixtures becomes clear when one considers that SAXS and spectroscopic studies of these systems demonstrate the existence of nanoscale order in water-saturated amine/acid mixtures corresponding to alternating hydrophobic and hydrophilic domains,[14] and thus an interface between them. Prior work[14] puts the characteristic length scale for such domains at roughly 15-18 Å for the systems considered here, implying an enormous surface-to-volume ratio for the resulting domains. While some ions such as alkali metals are known to be depleted at hydrophobic/hydrophilic interfaces,[24] experimental[25–27] and theoretical studies[24,28] suggest that soft ions accumulate at hydrophobic/hydrophilic interfaces to an extent that increases with their chaotropic character. The presence of such an interfacial area in the acid/amine mixtures discussed here suggests that the Hofmeister effect could draw ions from an isotropic, bulk aqueous phase to an "interfacially-rich" organic phase.

citrate ⇨ SO_4^{2-} ⇨ PO_4^{2-} ⇨ F^- ⇨ Cl^- ⇨ Br^- ⇨ I^- ⇨ NO_3^- ⇨ ClO_4^-

Figure 1: Hofmeister series for anions.

Apart from the original Hofmeister series, a number of headgroups have been ordered in a "Hofmeister-like" series, based on the principle of water affinities.[29] The carboxylic acid headgroup is described as "hard", whereas the amine headgroup is described as "soft".[30] In this work, the same headgroups have been used for all mixtures, to investigate exclusively the influence of anions present on the (lyotropic) Hofmeister series.

The molecular mechanism underlying the Hofmeister effect, with particular interest in the role of water affinity, has recently seen renewed interest.[29,31–35] However, the range of possible ionic species present in the extraction experiments reported here complicates such a molecular interpretation. Further, the presence of nanoscale liquid structure suggests that water present in the organic phase may be confined within hydrogen-bonding domains, leading to behavior quite different from that observed in bulk water. Considering these complications, this study focuses on the phenomenology of the Hofmeister effect and does not invoke its molecular interpretation.

Water content is a potentially important variable in understanding these systems. The presence of copper in the present study interferes with Karl-Fischer titration measurements.[36] Previous work measured water content via Karl-Fischer titration in water-saturated mixtures of this type, and indicates that it ranges from a mole fraction of 0.04-0.06 in the 3 amine/1 acid mole ratios to 0.2-0.3 in the 1 amine/3 acid mixtures.[14]

Aim of the study

This study seeks to characterize the connection between local liquid structure and extraction phenomena. To that end, we varied the composition of three amine/acid liquid mixtures and determined their extraction behavior for a series of aqueous copper salts with different anions from an aqueous phase. The organic phases were studied before and after extraction via SAXS to document the liquid structure and its changes.

Three copper salts ($Cu(NO_3)_2$, $CuCl_2$, and $CuSO_4$) were chosen for extraction. The set spans a range of positions in the Hofmeister series for the anions, and these anions do not coordinate strongly with copper in the aqueous phase,[37] eliminating a possible complicating factor in extraction equilibria. A set of anions were tested in an acid extraction study,[38] and it was shown that these anions follow the Hofmeister series.

These copper ions were extracted from aqueous phases to amine/acid mixtures. Prior work[14] indicated that for amine/acid mixtures of this type at a 1 amine:3 acid mole ratio, a well-developed nanoscale local liquid structure is observed, but when the amine:acid ratio is significantly less than 1:1, the structure is poorly-developed or unobserved. Consequently, we study these systems at 3 amine:1 acid, 1 amine:1 acid, and 1 amine:3 acid ratios (referenced as acid-poor, equimolar, and acid-rich, respectively).

The extent of extraction for both the cations and anions of the copper salt was measured by ICP, allowing inference of the relative importance of the mechanisms reported in Table 1. The water-saturated protic mixtures used in the extraction experiments, and the organic phases resulting from the extraction experiments, were examined via SAXS.

Methodology:

For the extraction experiments, trihexylamine (96%), trioctylamine (98%), octanoic acid (98%), decanoic acid (>99.5%), oleic acid (99%), copper nitrate (99.99%), copper II chloride (99.999%) and copper sulfate (99.999%) were purchased from Sigma Aldrich and used as received. Milli-Q water (18.2 MΩ) was used to prepare the metal solutions. The protic mixtures were prepared by mixing the respective amine and acid in 1:1, 3:1 and 1:3 molar ratios using a vortex for 1 hour. The mixture was left resting overnight. $Cu(NO_3)_2$, $CuCl_2$ and $CuSO_4$ solutions were prepared in concentrations of 50, 100 and 200 mM.

3 grams of the protic mixture and 3 grams of copper solution were put in a 15 mL centrifuge tube and mixed using a Vortex Genie II for 30 minutes. The mixture was

centrifuged using a Hettich 380R centrifuge to obtain phase separation. The phases were separated using disposable needles and syringes. The copper concentrations were analyzed using a Spectro-Arcos ICP-OES. A Dionex DV4500 ion chromatograph was used to analyze the nitrate, chloride and sulfate concentrations. Water measurements were conducted using a Karl-Fischer coulometer (Metrohm 756 Coulometer).

Preparation of samples for SAXS experiments were prepared in a different laboratory and followed a slightly different protocol; see Supplementary Material for details.

SAXS measurements were done on a SAXSLabs (Amherst, MA) custom instrument equipped with Bruker AXS copper rotating anode and PILATUS 300K area detector. The detector's nominal position varied from ~0.2 to 1.5 meters depending on the scattering vector range investigated; the actual detector position was calibrated with silver behenate. For SAXS experiments samples were placed in 1 mm glass capillaries (Charles Supper, MA) and sealed. The data reduction from 2D to 1D was done on Saxsgui software (saxsgui.com). The 1D SAXS data were fit using Mathematica 11 (Wolfram Research).

Results & Discussion:

The mixtures of interest are given in Table 2 and consist of three different tertiary amines in combination with three different acids. The tertiary amines and acids cover a broad spectrum in terms of hydrophobicity.

Code	Amine	Acid
A	Trihexylamine	Octanoic acid
B	Triocytlamine	Decanoic acid
C	Trioctylamine	Oleic acid

Liquid systems are denoted by the letter code followed by numbers giving the amine:acid ratio. Thus

A13: Mixture A with a 1 amine:3 acid mole ratio,

C11: Mixture C with a 1 amine:1 acid mole ratio, etc.

Table 2: Notation for liquid mixtures used in this research.

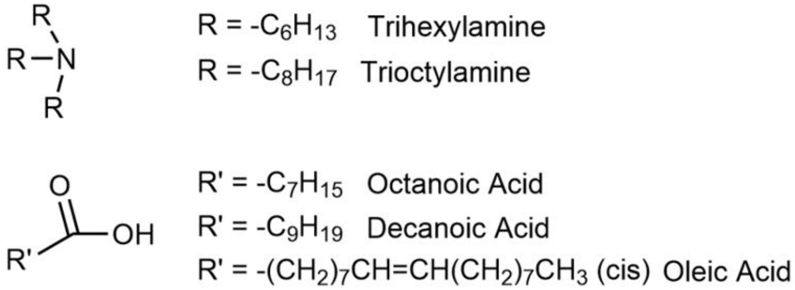

Figure 2: Structures of the amines and acids used in this study.

A central variable in the present experiments is the amine/acid mole ratio, ranging from 3 amine/1 acid to 1 amine/3 acid.

A. Trihexylamine/Octanoic Acid Protic Mixtures:

The results for the extractions to trihexylamine/octanoic acid (A-series) are shown in Figure 3. At almost every concentration, the extraction efficiency of copper is greatest for the nitrate salt and least for the sulfate ion, which is consistent with the Hofmeister series. The sole exception is for the low concentration extraction in A13, where the copper extraction efficiency is slightly higher for the sulfate salt than for the chloride.

In most cases the extraction efficiencies of the copper and nitrate ions are nearly equal, indicating that neutral extraction is the dominant mechanism. For the A31 cases, however, the cation exchange mechanism appears significant for $CuCl_2$ and $CuSO_4$. In contrast, for the A13 case, anion exchange appears significant for high concentrations of $CuSO_4$. A definitive explanation for the variation in exchange mechanism as a function of amine/acid ratio cannot be provided.

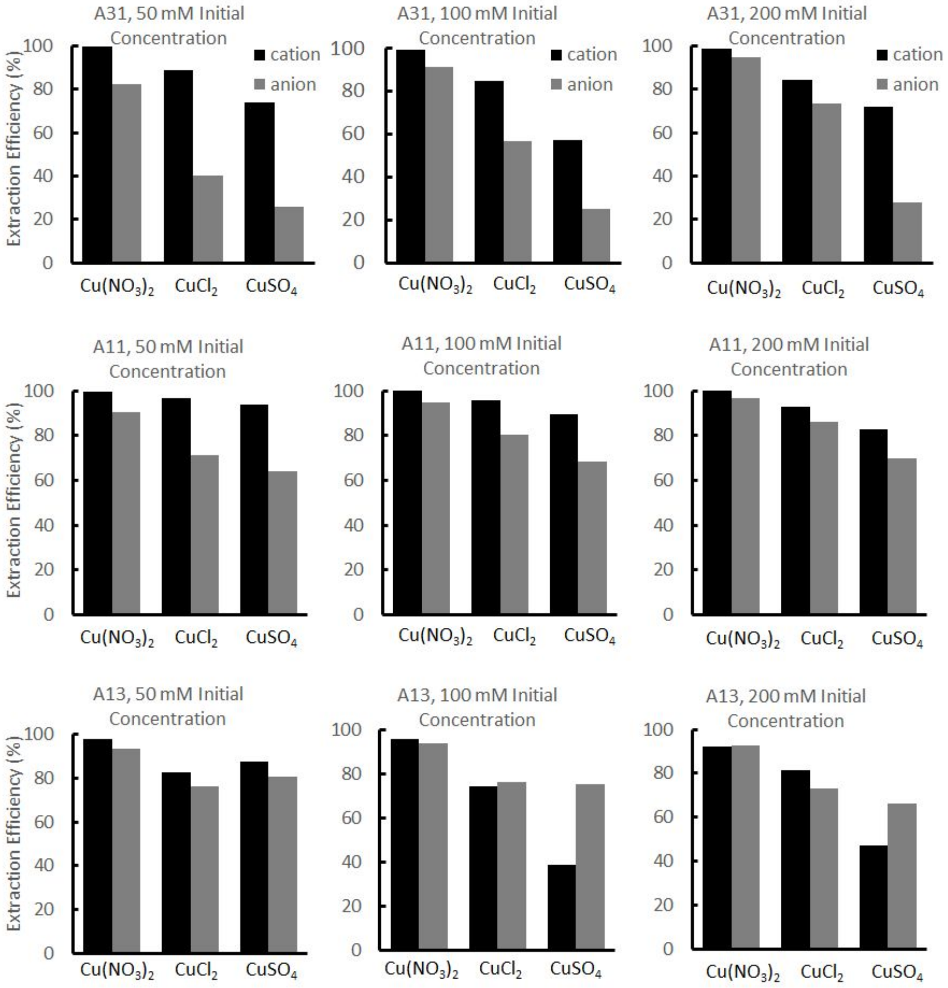

Figure 3: Extraction results for trihexylamine/octanoic acid mixtures in varying amine:acid ratio (A-series). For each salt, the cation extraction efficiency is shown in black and the anion extraction efficiency is shown in gray. Amine/acid mole ratio varies along each column, and initial copper salt concentration in the aqueous phase varies along each row.

When only the extent of anion extraction is considered, the Hofmeister effect is obeyed in almost every case (i.e. the extent of extraction is greatest for nitrate and least for sulfate). Again, the sole exception is the low concentration A13 case.

This second trend is clear when one compares the extent of the extraction of nitrate anion vs. sulfate anion, which is a measure of the extent to which the Hofmeister effect operates under different conditions. We define the strength of the Hofmeister effect for anions as follows:

$$\sigma=(\text{Extraction efficiency of nitrate ions}) - (\text{Extraction efficiency of sulfate ions})$$

σ-values as a function of the amine-acid ratio are shown in Figure 4. The strength of the Hofmeister effect is greatest in the acid-poor (A31) mixtures and least (on average) in the acid-rich (A13) mixtures. The variation of σ with initial copper salt concentration in the acid-rich (A13) mixtures correlates with a shift from a predominantly neutral extraction mechanism for $CuSO_4$ at low concentrations to an anion exchange mechanism at high concentrations.

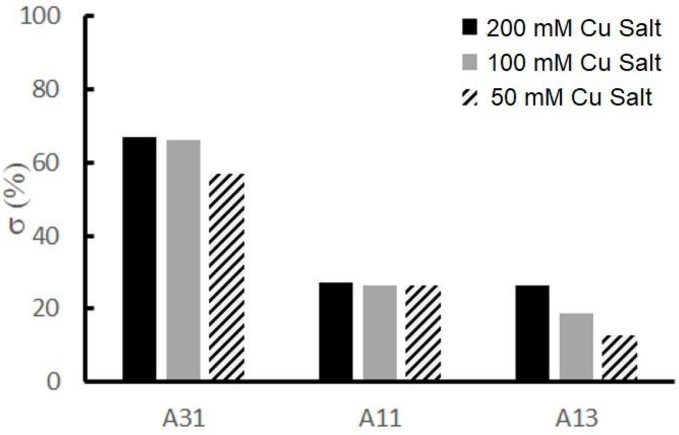

Figure 4: σ as a function of amine/acid ratio and initial copper salt concentration for the trihexylamine/octanoic acid system.

The strength of the Hofmeister effect in these extraction experiments correlates with the results of the SAXS profiles of the organic phases as described below. First a representative plot of the A31 control experiment (without copper salt extraction but water saturated) showing the full range of the SAXS data is given in Figure 5, along with the fitting curves used in the analysis.

A peak in the scattering wavenumber q on the horizontal axis is associated with a characteristic lengthscale $D=2\pi/q$ within the liquid. Previous SAXS studies[14] of the water-saturated mixtures assigned the peak near $q=1.4$ Å^{-1} to intramolecular distances associated with the alkyl chains, consistent with similar distances observed in liquid hydrocarbons[39] and polyethylene polymers[40] and with studies involving ionic liquids with long, aliphatic side-chains.[41] The peak near $q=0.4$ Å^{-1} was identified as resulting from a nanoscale local liquid structure emerging from the hydrogen-bonding interactions of the acid, the amine, and the water molecules. For the A31-series, the peak representing the local structure is well-described by a single Lorentzian feature, though there is a shoulder near q=0 that requires the use of an “off-plot” Lorentzian to describe it; the origin of this structure is discussed below.

Throughout the paper we make reference to “structure,” but we wish to clarify what that means in this context. Physicochemical studies[9,10,14] indicate the existence of a hydrogen-bonding network in these species which is best developed at liquid compositions where the low-q SAXS peak is best-developed. The likeliest explanation for this correlation is that the hydrogen-bonding network leads to segregation of polar groups (including amine nitrogens, carboxylic acid groups, water and ions accumulated in solvent extraction) and aliphatic groups in the organic phase. The 15-20 Å characteristic lengthscales of these features are broadly consistent with molecular sizes (see supporting information, Figure S5, Table S1), however the exact molecular arrangement in the structure is still unclear and warrants additional investigation. This does not necessarily imply that the observed SAXS features are well-defined structures analogous to those of, for example, micelles in water. All that can be inferred from the SAXS signals is the existence of liquid order with certain characteristic lengthscales. We refer to this as “liquid structure,” with the proviso that it may include configurations of widely varying shape and composition.

In Figure 6 we report the results of SAXS experiments for the organic phase associated with the 100 mM initial copper salt concentration extraction experiments, representing the region of q values up to 1 that are associated with the nanoscale local liquid structure in Figure 5, along with
a water-saturated sample of the protic mixture as a control. Full SAXS data for all systems and a description of the fitting procedure is reported in the Supplementary Information.

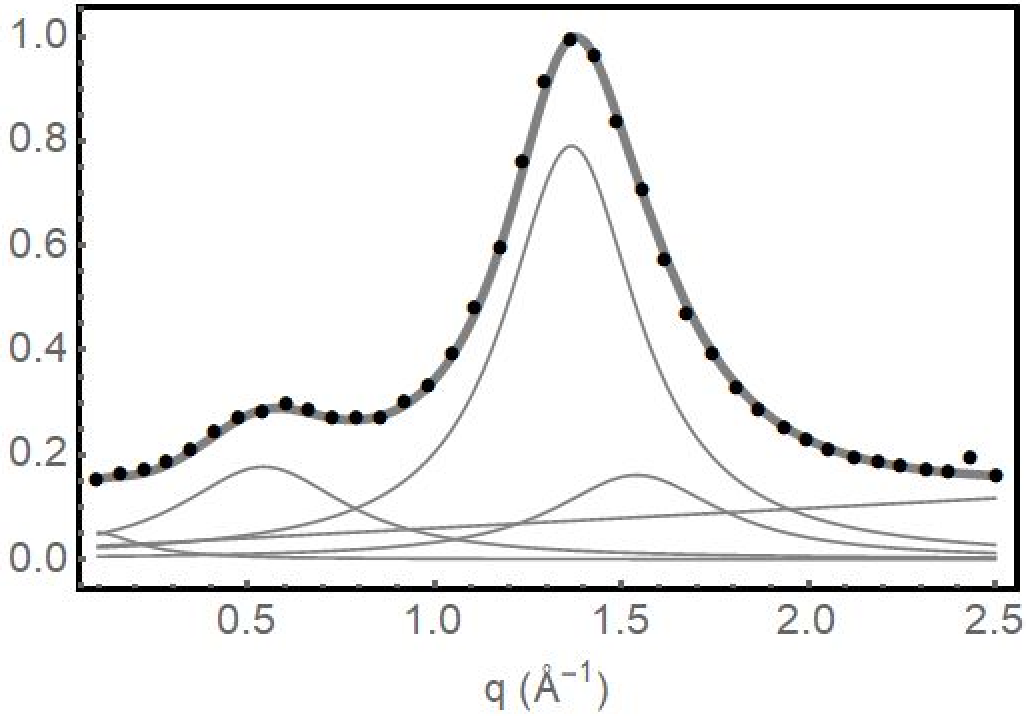

Figure 5: Experimental (black dots) and fitted (heavy gray line) SAXS data for the A31 water blank experiment. Only every 10th experimental datapoint is shown to improve readability. Light gray lines show components of fit (four Lorentzian curves and a linear baseline).

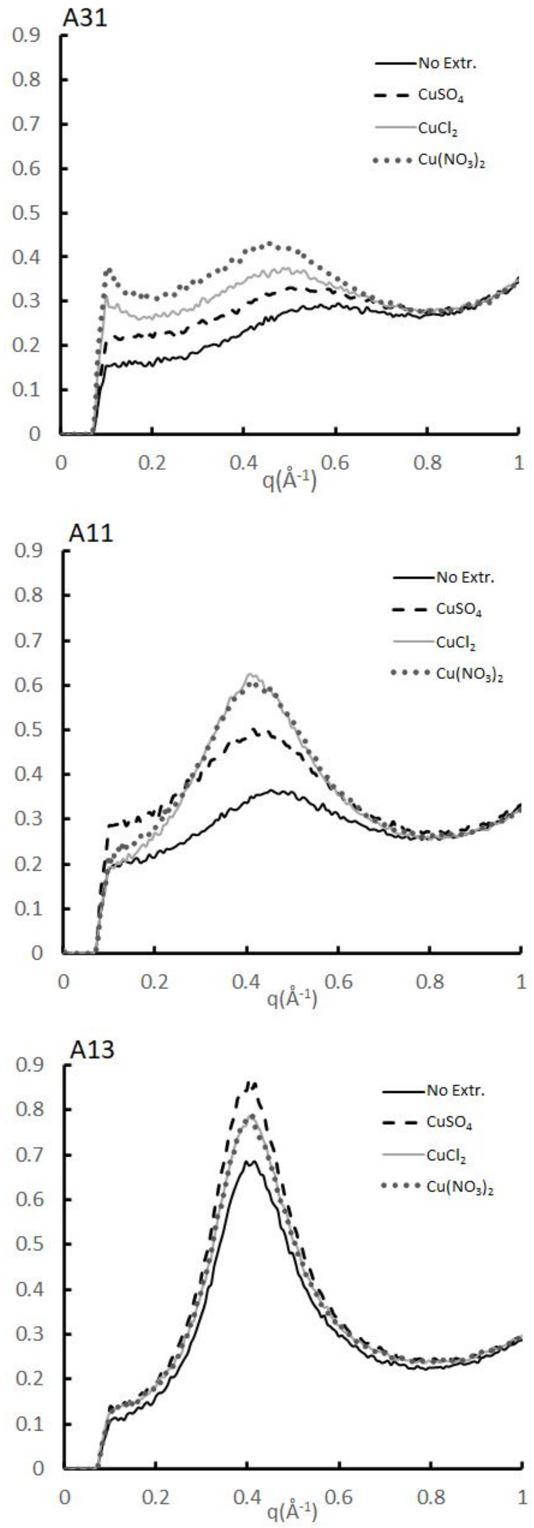

Figure 6: SAXS results for low-q region of trihexylamine/octanoic acid mixtures after extraction from 100 mM stock solution. Top: 3 Amine:1 Acid; Center: 1 Amine:1 Acid;

Bottom: 1 Amine:3 Acid. Signals are normalized against the peak near q=1.5 Å^{-1} to facilitate comparison.

Mixture	Experiment	Nanostructure Peak Maximum (Fit)		Nanostructure Peak Width (Fit)
		q(Å^{-1})	D(Å)	w(Å^{-1})
A31	Blank	0.543	11.6	0.270
	$CuSO_4$	0.512	12.3	0.287
	$CuCl_2$	0.472	13.3	0.272
	$Cu(NO_3)_2$	0.451	13.9	0.246
A11	Blank	0.455	13.8	0.245
	$CuSO_4$	0.423	14.9	0.218
	$CuCl_2$	0.416	15.1	0.165
	$Cu(NO_3)_2$	0.417	15.1	0.178
A13	Blank	0.400	15.7	0.086
	$CuSO_4$	0.396	15.9	0.087
	$CuCl_2$	0.401	15.7	0.089
	$Cu(NO_3)_2$	0.397	15.8	0.088

Table 4: Peak maximum and width for nanoscale feature for A-series mixtures as a function of amine/acid ratio and extraction experiment. Fitting procedures as described in the SI.

The results of fitting the low-q peak to a single Lorentzian are given in Table 4; these serve to quantify comparisons between the experiments. For the A13-series feature, the asymmetry of the peak requires a second, relatively small Lorentzian feature near q=0.51

Å^{-1} to describe it; the small amplitude of this contribution means it does not significantly affect peak center or width. Details are given in the SI.

One further point that must be addressed is the rising shoulder for q<0.2 Å^{-1} for the A31Cl and A31NO$_3$ cases. This was explored by additional SAXS experiments using longer exposure times at low q; details are reported in the SI. The shoulder implies the existence of larger-scale entities within the liquid that are absent in the analogous A11 and A13 experiments.

The exact nature of these regions cannot be determined from our experiments. However, as discussed in the SI, the signal is well-modeled as the scattering of polydispersed, spherical particles with a most probable size of 5 nm. Interestingly, the observed domain size does not change between the chloride and nitrate cases, but the contribution to the scattering from these heterogeneities is higher in the case of the nitrate salt. This could be due either to a higher concentration of the minor domain entities or increased contrast between the two phases.

Given that these entities appear only in the acid-poor nitrate- and chloride-containing species, it is possible that these structures involve the creation of some form of hydrophobic/hydrophilic interface that is stabilized by the chaotropic anions. However, the composition of the observed entities cannot be determined from the SAXS experiments and as these observations are of secondary importance to this work we refrain from further speculation.

Considering first trends between different groups, the value of q generally decreases running from A31 to A13, corresponding to an increase in lengthscale. Peak width decreases in the same trend, suggesting a decrease in polydispersity associated with the observed structures. This is consistent with observations in earlier work[14] that the local liquid structure of these systems is best-developed at a mole ratio of 1 amine:3 acid. The hydrogen-bonding network associated with the observed SAXS structure is most fully developed when the amine:acid mole ratio is 1:3. Under these conditions, the structure is unaffected by the presence of the copper salts, as evidenced by the invariance in both lengthscale and polydispersity for the A13-series.

Turning now to the trend within each series, we note that for the A31 and A11 experiments the q value for the peak maximum systematically decreases in the series Blank>SO_4>Cl>NO_3 (though A11Cl and A11NO_3 are nearly identical). This corresponds to an increase in characteristic lengthscale D that correlates with the chaotropic character of the anion. It can also be observed that the width of these features w generally decreases as the lengthscale increases, though A11Cl and A11NO_3 are again an exception. The hydrogen-bonding nanostructure is poorly developed in the water blank of the A31-series, where the mole ratio inhibits its emergence.

While this is a more complex system than the surfactant systems noted in the introduction, the observed changes in local structure do seem driven by the Hofmeister effect in a manner loosely analogous to the structural changes observed for the critical micelle concentration in electrolytes. This should not be taken to imply any particular morphology of the local structure in the amine/acid mixtures. We make the point merely to emphasize that the variation of the local structure with the chaotropic character of the anion is similar to phenomena observed in other contexts.

Whatever the nature of the structure, it appears well-developed in the A13-series, even in the absence of the extracted salts. This may explain why there is no significant change in the local liquid structure after extraction, as these structures may already be in some relatively stable configuration and so are robust with respect to interactions with the chaotropic anions.

We note that the above discussion neglects a possible role for the copper ion in promoting the emergence of local liquid structure. The copper ion is known to be relatively chaotropic,[42] but some caution is in order when attempting to understand its surface-specific effects. As Gao and co-workers note, the presence of strong Lewis bases can lead to complex coordination structures that influence ionic hydration.[42] This parameter is known to be important to the Hofmeister effect. Given that copper is known to coordinate strongly with amines[43,44] and carboxylates,[44–46] it is difficult to predict how the presence of the copper will influence local liquid structure or, indeed, whether it will have a stronger influence through its chaotropic character or through its coordination behavior.

The correlation between liquid structure and the strength of the Hofmeister effect is worth considering. The identity of the anion is a significant determinant of the local structure of the liquid for the A31-series of liquids, but has little effect on the A13-series. This implies that the solute-solvent interaction energies responsible for nanoscale structural changes in the A31 liquid are more sensitive to the identity of the anion than those of the A13 series. This inference is consistent with the observation that the σ parameter describing the strength of the Hofmeister effect is largest for the A31-series and least for the A13 series, as the solute-solvent interactions should influence both liquid structure and extraction efficiency.

In other words, the extraction efficiency is coupled to local nanoscale liquid structure by the Hofmeister effect. While the Hofmeister effect often plays a role in extraction phenomena, the present results are significant in that they correlate the action of the Hofmeister effect with specific SAXS observations of a bulk liquid. Further, the relevant solute-solvent interactions in the present case are distinct from those observed in liquids lacking nanoscale structure, and their sensitivity to liquid composition suggests a strategy for controlling the strength of the Hofmeister effect. This represents a degree of freedom that could be used in the optimization of selective extraction processes.

No further insight on the nature of the liquid structure peak can be offered. However, both the shape and maximum of the peaks vary significantly both within the compositions of each reported mixture and cross the different mixtures.

B. Trioctylamine/Decanoic Acid Mixtures

The results of extraction experiments for the 1 trioctylamine:3 decanoic acid ratio are not reported, as the extraction process led to the formation of precipitates in the $Cu(NO_3)_2$ and $CuCl_2$ cases. The extraction efficiencies for 1:1 and 3:1 amine:acid ratios are presented in Figure 7. With the exception of the B31 $CuSO_4$ experiment, the extraction efficiencies of the copper ion and the anion are nearly equal in all cases. This indicates that neutral extraction is the dominant mechanism, as in most A-series experiments.

The B31-series extraction experiments are consistent with the Hofmeister series, though this is not the case for the B11-series where the extraction of $CuCl_2$ is lower than would be expected based on the Hofmeister series. The value of σ is lower for B11 than for B31, consistent with the pattern observed for the A-series experiments.

This anomaly correlates with an anomaly in the SAXS experiments (figure 9), with fitting data reported in Table 5. For the B11-series extraction experiments, the feature associated with the local structure peaks is at ~0.36 $Å^{-1}$ in every case. However, the peak for the chloride extraction is significantly narrower than for either of the other extractions, possibly indicating a better-defined structure. This may be the result of some idiosyncrasy in the interactions between the medium and the chloride ion, but we have no detailed explanation and refrain from further speculation.

Other than this anomaly, the results of the B-series extractions and SAXS experiments are consistent with the interpretation of the A-series experiments offered above. In particular, both the extraction efficiency and the characteristic lengthscale for the B31 mixture are very sensitive to the chaotropic character of the anion. The structure of the B11 liquid appears largely independent of anion identity, and the extraction efficiency varies only weakly with the identity of the anion, albeit in violation of the Hofmeister series noted above. Thus, while the situation is complex, it is broadly consistent with the earlier discussion about the coupling between local liquid structure and the observed solvent extraction efficiencies in Part A of the Results above.

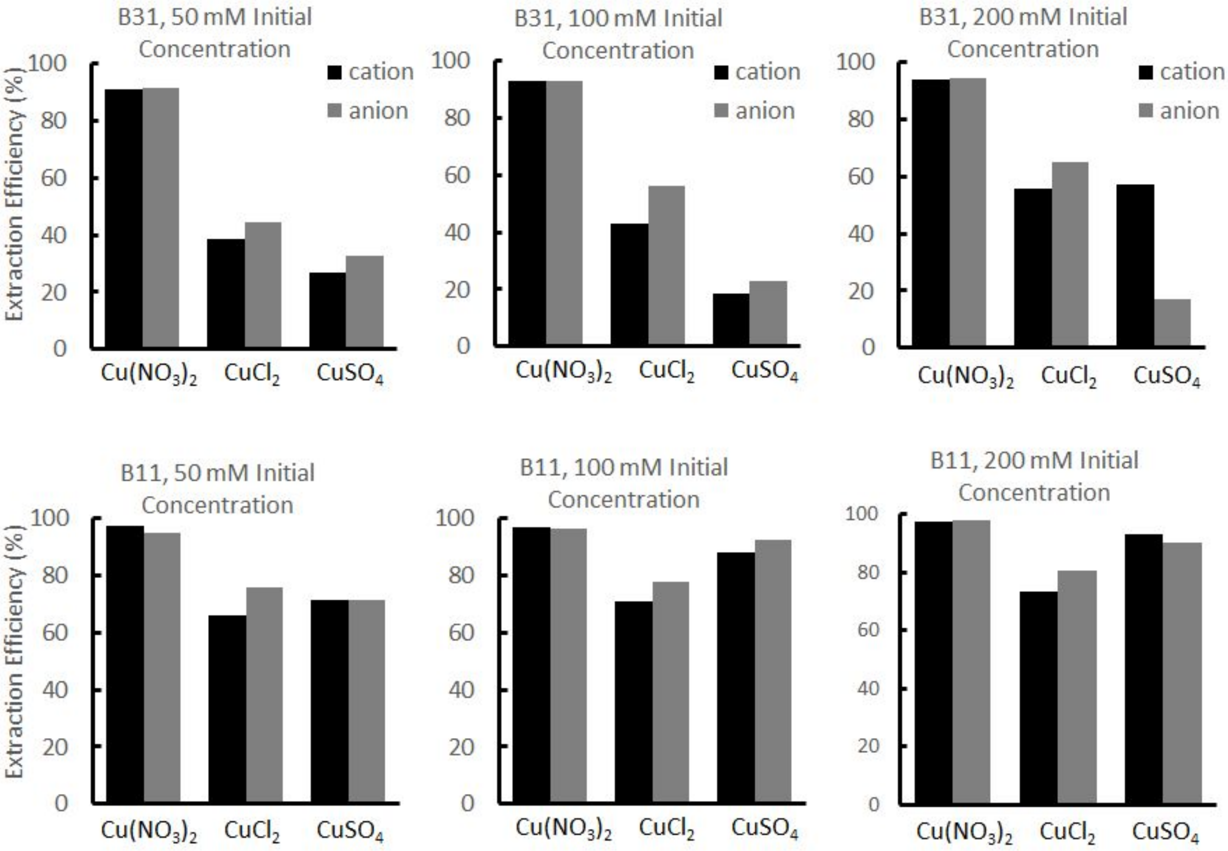

Figure 7: Extraction results for trioctylamine/decanoic acid mixtures in varying amine:acid ratio (B-series). For each salt, the cation extraction efficiency is shown in black and the anion extraction efficiency is shown in gray.

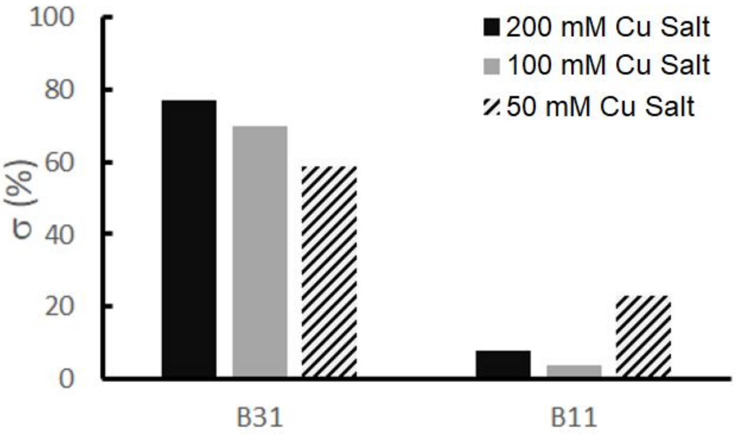

Figure 8: σ as a function of amine/acid ratio and initial copper salt concentration for the trioctylamine/decanoic acid system.

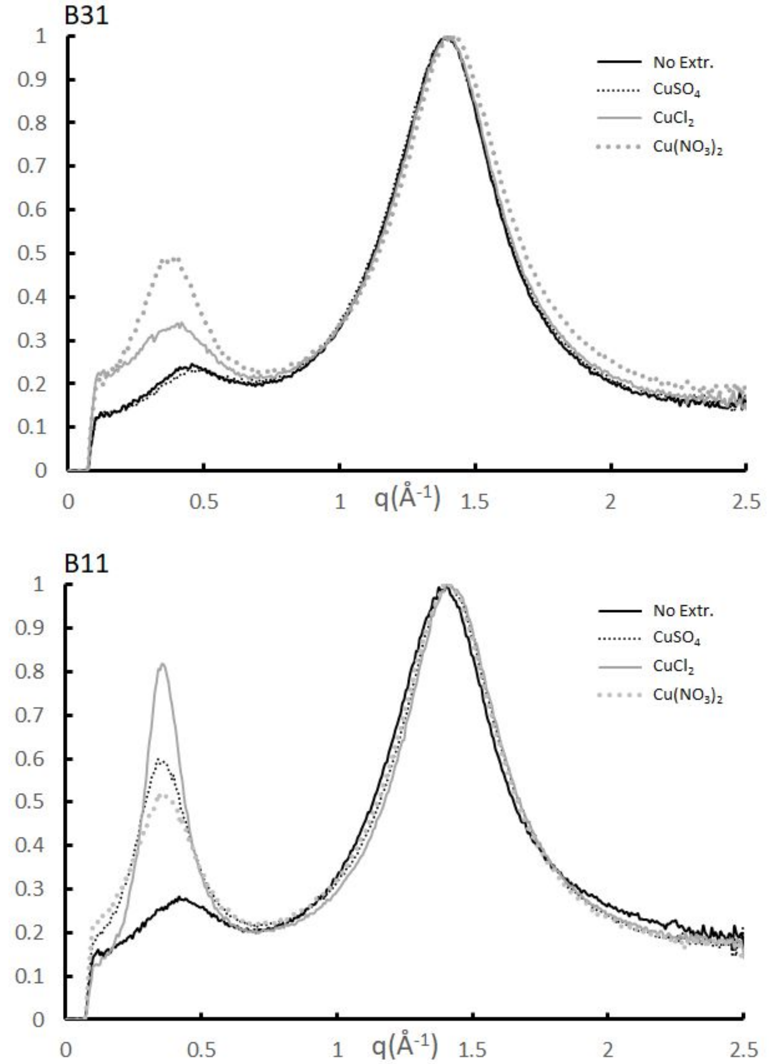

Figure 9: SAXS results for low-q region of trioctylamine/decanoic acid mixtures after extraction from 100 mM stock solution. Top: 3 Amine:1 Acid; Center: 1 Amine:1 Acid; Bottom: 1 Amine:3 Acid. Signals are normalized against the peak near q=1.5 Å^{-1} to facilitate comparison.

Mixture	Experiment	Nanostructure Peak Maximum (Fit)		Nanostructure Peak Width (Fit)
		q(Å^{-1})	D(Å)	w (Å^{-1})
B31	Blank	0.434	14.5	0.169

	$CuSO_4$	0.451	13.9	0.173
	$CuCl_2$	0.389	16.2	0.177
	$Cu(NO_3)_2$	0.372	16.9	0.145
B11	Blank	0.405	15.5	0.186
	$CuSO_4$	0.356	17.6	0.125
	$CuCl_2$	0.357	17.6	0.087
	$Cu(NO_3)_2$	0.357	17.6	0.150

Table 5: Peak maximum and width for nanoscale feature for B-series mixtures as a function of amine/acid ratio and extraction experiment. A graphical presentation of the SAXS data and the fitting procedures are described in the SI.

C. Trioctylamine/Oleic Acid Mixtures:

The extraction efficiencies for the trioctylamine/oleic acid mixtures are reported in Figure 10. The $Cu(NO_3)_2$ samples display high extraction yields and comparable cation and anion extraction efficiencies, suggestive of the dominance of neutral extraction and consistent with observations for the other solvent systems. Cation exchange appears to be an important contributor for high initial concentration extractions for $CuSO_4$ in the C31 and C13 cases, similar to that observed in A31.

The presence of significant cation exchange breaks the correlation between Cu^{2+} extraction and the Hofmeister effect. However, the extraction efficiencies of the anions obey the Hofmeister series in almost every case, with the exception being the low concentration C13 case; a similar exception is observed in the low concentration A13 experiments. The trend in σ is consistent with the other cases, with σ being largest for the C13 series and smallest for the C31 series (though the high concentration C11 experiments violate the trend). Thus, despite the complications arising from the prevalence of non-neutral extraction mechanisms, the Hofmeister effect continues to play an important role in the process.

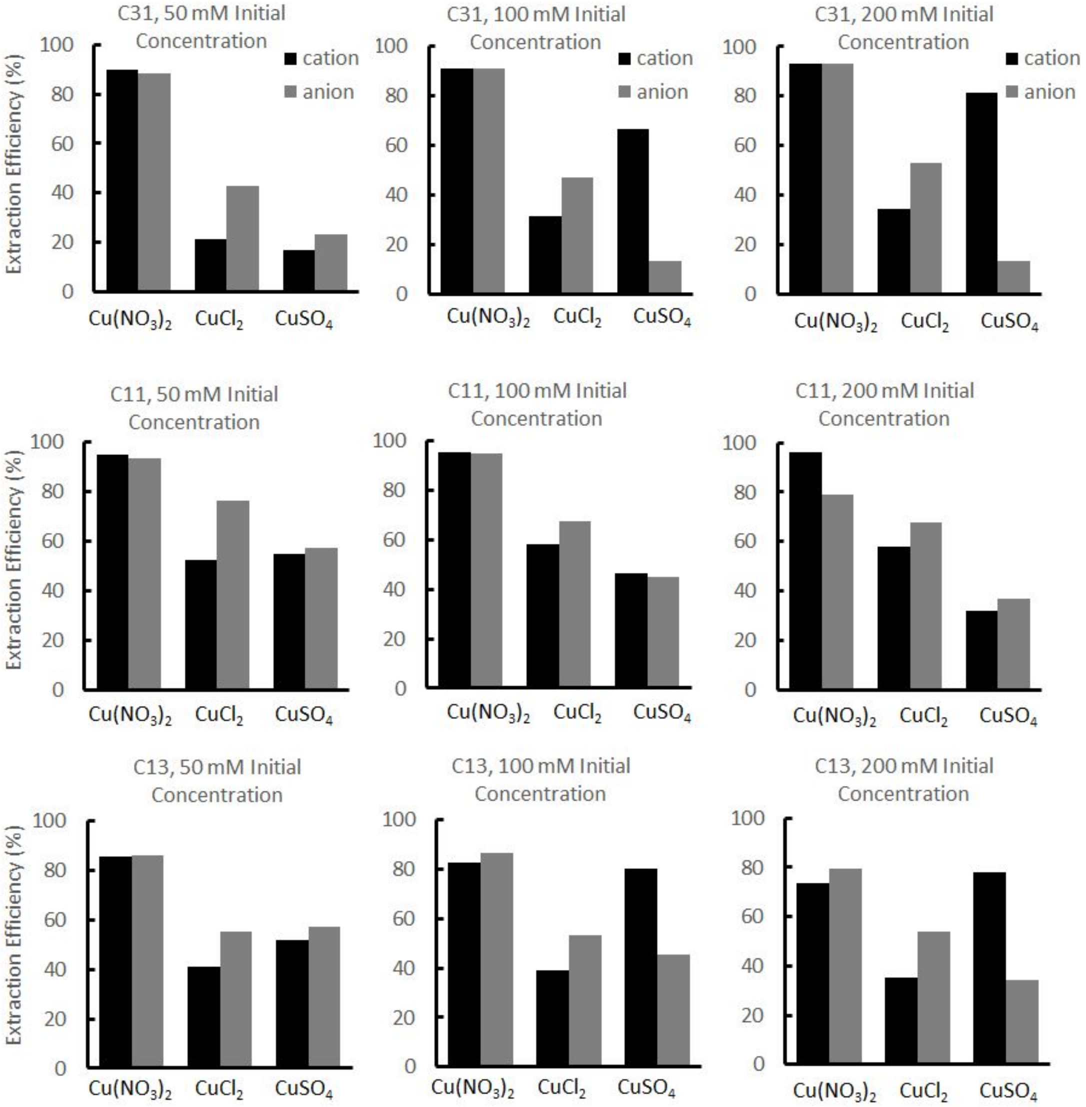

Figure 10: Extraction results for trioctylamine/oleic acid mixtures in varying amine:acid ratio (C-series). For each salt, the cation extraction efficiency is shown in black and the anion extraction efficiency is shown in gray. Amine/Acid mole ratio varies along each column, and initial copper salt concentration in the aqueous phase varies along each row.

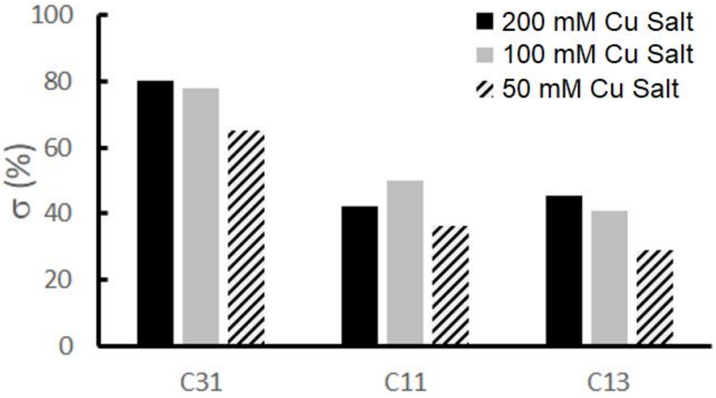

Figure 11: σ as a function of amine/acid ratio and initial copper salt concentration for the trioctylamine/oleic acid system.

The SAXS results are given in Figure S3 in the SI and in Figure 12. For these systems, the low-q features associated with the local structure require two Lorentzian peaks to model, making analysis based on tabular data impractical. Inspection of the peaks indicates that the feature is broadest for the C31-series and narrowest for the C13-series. It is also tempting to infer that the center of the feature shifts to lower *q*-values (higher *D*-values) moving from C31 to C13, but the breadth and complexity of the features make it difficult to state this definitively. Regardless, the observed narrowing of the peaks is consistent with the idea that local structure is best developed for the C13 case.

Trends within each series are also consistent with those observed in the A-series cases. The nanostructure feature shifts to lower *q* in the C31-series as one moves along the Hofmeister series from sulfate to nitrate in the C31-series. And in the C11Cl and C11NO_3 cases the distribution is significantly narrower than in the C11SO_4 and C11 Blank cases. Both of these trends are consistent with their A-series analogs, and the relatively limited variation in structure observed in the C13-series is similar to that in the A13-series.

As in the A-series and B-series results, the correlation between the sensitivity of liquid structure to anion identity and the variation in σ indicate that the solute-solvent interactions responsible for changes in nanoscale liquid structure are coupled to extraction equilibria.

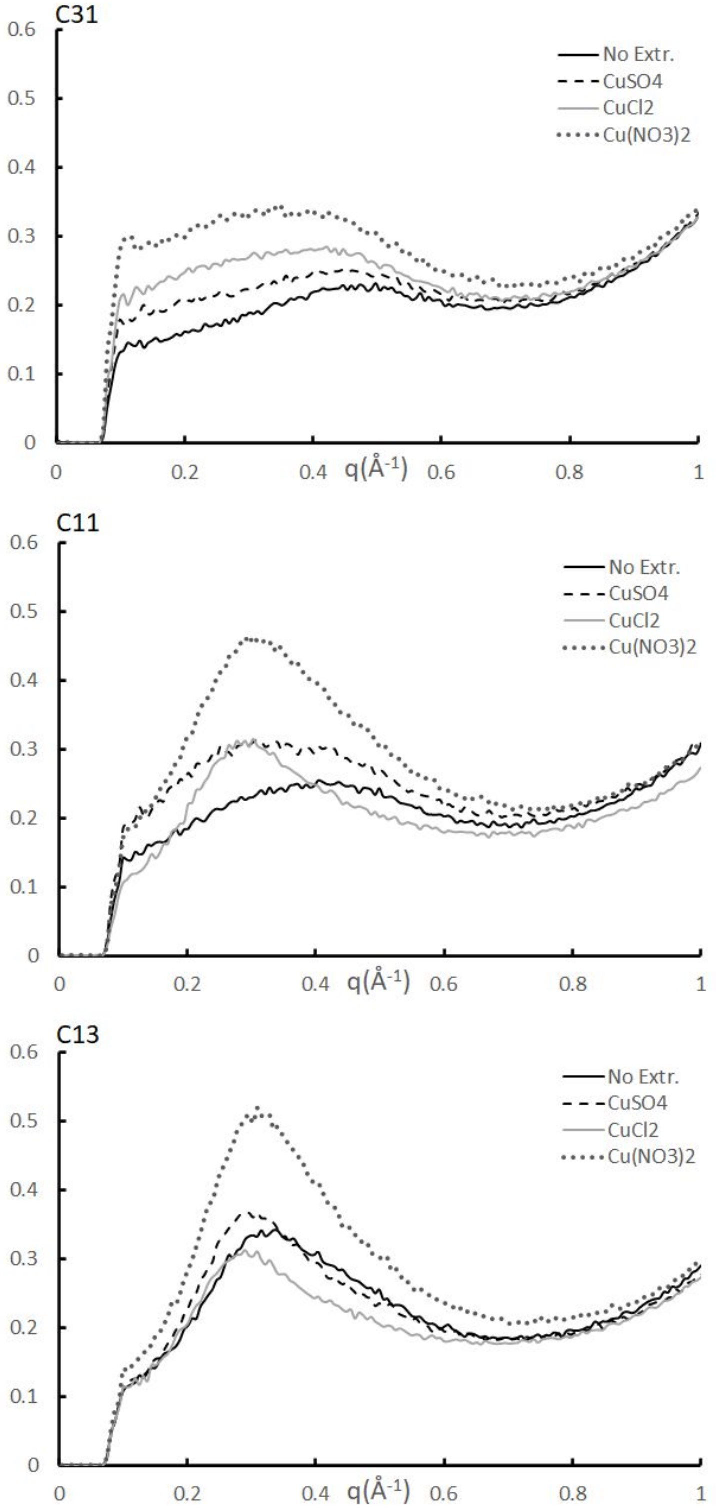

Figure 12: SAXS results for low-q region of trioctylamine/oleic acid mixtures after extraction from 100 mM stock solution. Top: 3 Amine:1 Acid; Center: 1 Amine:1 Acid;

Bottom: 1 Amine:3 Acid. Signals are normalized against the peak near q=1.5 Å^{-1} to facilitate comparison.

Conclusions:

A close connection between the nanoscale local structure of an amine/acid liquid mixture and its behavior as a medium for liquid-liquid extraction of copper salts from aqueous phase has been demonstrated. The size and character of these structures as observed by SAXS change during the extraction in ways that correlate with the Hofmeister character of the anion, and these changes offer insight on how the Hofmeister effect influences the extraction process.

In 1 amine:3 acid mole ratio mixtures, the nanostructure is well-developed owing to a well-developed hydrogen-bonding network. Under these conditions the liquid structure remains relatively unchanged by the uptake of the copper salts, and the Hofmeister effect of the anions is relatively weak.

In contrast, for the 3 amine:1 acid mixture the hydrogen-bonding nanostructure was poorly-defined in the absence of an extracted salt, and both the short-range order and the emergence of long length scale structures depended heavily on the chaotropic nature of the anion and its position in the Hofmeister series.

The study makes clear that the Hofmeister effect couples extraction equilibria to the solute-solvent interactions that influence nanoscale liquid structure. In most organic solvents there is a substantial free energy cost to transporting hydrophilic inorganic anions from an aqueous phase to a more hydrophobic organic medium. However, the presence of nanoscale liquid structure in the organic phase of the present system brings the Hofmeister effect into play, with ions apparently being drawn to the interface. The strength of the coupling between liquid structure and extraction behavior depends on liquid composition, meaning that it can be tuned to the needs of a particular process.

Outlook

The fact that the nature of the nanoscale liquid structure can be controlled by varying the amine/acid mole ratio offers an intriguing new approach to the optimization of extraction processes. For example, it may be possible to use a well-chosen solvent composition to preferentially extract specific combinations of cation and anion with chaotropic or kosmotropic character. This approach is markedly different from the most metal extraction approaches, which are based on the coordination chemistry of the metal and the hydrophobicity of a chelating agent. Combining these approaches may open novel avenues to metal separations.

Acknowledgments:

The authors would like to thank Michel van den Brink for the fruitful discussions and his help with the analyses and Rocío Aguirre Dominguez and Iván Perez Solares for their help with a number of extraction experiments. This work was supported by UNAM-PAPIIT IA103619 (“Programa de Apoyo a Proyectos de Investigación e Innovación Tecnológica”) and by the “Programa de Apoyo a la Investigación y el Posgrado de la Facultad de Química UNAM” (PAIP 5000-9175). We gratefully acknowledge financial support for this project through a grant from the Professional Staff Congress of the City University of New York. This research used resources of the Center for Functional Nanomaterials, which is a U.S. DOE Office of Science Facility, at Brookhaven National Laboratory under Contract No. DE-SC0012704.

Conflicts of interest

The authors would like to state that there is no conflict of interest.

Bibliography:

1 T. Welton, Ionic liquids: a brief history, *Biophys. Rev.*, 2018, **10**, 691–706.

2 A. E. Visser, R. P. Swatloski, W. M. Reichert, H. D. Willauer, J. G. Huddleston and R. D. Rogers, Room temperature ionic liquids as replacements for traditional organic solvents and their applications towards ‘green chemistry’ in separation processes, *NATO Sci. Ser., II*, 2003, **92**, 137–156.

3 B. Braibant, D. Bourgeois and D. Meyer, Three-liquid-phase extraction in metal recovery from complex mixtures, *Sep. Purif. Technol.*, 2018, **195**, 367–376.

4 M. Herrero, J. A. Mendiola and E. Ibáñez, Gas expanded liquids and switchable solvents, *Curr. Opin. Green Sustain. Chem.*, 2017, **5**, 24–30.

5 C. H. C. Janssen, N. A. Macías-Ruvalcaba, M. Aguilar-Martínez and M. N. Kobrak, Copper extraction using protic ionic liquids: Evidence of the Hofmeister effect, *Sep. Purif. Technol.*, 2016, **168**, 275–283.

6 A. Eyal and A. Baniel, Extraction of Strong Mineral Acids by Organic Acid-Base Couples, *Ind. Eng. Chem. Process Des. Dev.*, 1982, **21**, 334–337.

7 A. M. Eyal, in *Solvent Extraction and Ion Exchange, vol. 13*, eds. J. A. Marinsky and Y. Marcus, Marcel Dekker, Inc., New York, 1997, pp. 31–93.

8 C. H. C. Janssen, M. C. Kroon, S. J. Metz, J. Van Spronsen and G. Witkamp, Extraction of Sodium Chloride from Water and Solubility of Water in Hydrophobic Trialkylammonium Alkanoate-Based Ionic Liquids, 2010, 3391–3394.

9 F. Kohler, H. Atrops, H. Kalali, E. Liebermann, E. Wilhelm, F. Ratkovics and T. Salamon, Molecular interactions in mixtures of carboxylic acids with amines. 1. Melting curves and viscosities, *J. Phys. Chem.*, 1981, **85**, 2520–2524.

10 F. Kohler, R. Gopal, G. Goetze, H. Atrops, M. A. Demeriz, E. Liebermann, E. Wilhelm, F. Ratkovics and B. Palagyi, Molecular interactions in mixtures of carboxylic acids with amines. 2. Volumetric, conductimetric, and NMR properties, *J. Phys. Chem.*, 1981, **85**, 2524–2529.

11 T. L. Greaves and C. J. Drummond, Protic Ionic Liquids: Evolving Structure–Property Relationships and Expanding Applications, *Chem. Rev.*, 2015, **115**, 11379–11448.

12 C. H. C. Janssen, Prevailing mechanisms in pseudo-protic ionic liquid metal extractions, *J. Mol. Liq.*, 2020, **304**, 112738.

13 H. Watanabe, T. Umecky, N. Arai, A. Nazet, T. Takamuku, K. R. Harris, Y. Kameda, R. Buchner and Y. Umebayashi, Possible Proton Conduction Mechanism in Pseudo-Protic Ionic Liquids: A Concept of Specific Proton Conduction, *J. Phys. Chem. B*, 2019, **123**, 6244–6252.

14 M. N. Kobrak and K. G. Yager, X-Ray scattering and physicochemical studies of trialkylamine/carboxylic acid mixtures: nanoscale structure in pseudoprotic ionic liquids and related solutions, *Phys. Chem. Chem. Phys.*, 2018, **20**, 18639–18646.

15 F. Hofmeister, Zur Lehre von der Wirkung der Salze, *Arch. Experim. Path. Pharmak.*, 1888, **24**, 247–260.

16 A. M. Hyde, S. L. Zultanski, J. H. Waldman, Y.-L. Zhong, M. Shevlin and F. Peng, General Principles and Strategies for Salting-Out Informed by the Hofmeister Series, *Org. Process Res. & Dev.*, 2017, **21**, 1355–1370.

17 J. M. Roberts, A. R. Diaz, D. T. Fortin, J. M. Friedle and S. D. Piper, Influence of the Hofmeister series on the retention of amines in reversed-phase liquid chromatography, *Anal. Chem.*, 2002, **74**, 4927–4932.

18 E. Leontidis, Investigations of the Hofmeister series and other specific ion effects using lipid model systems, *Adv. Colloid Interface Sci.*, 2017, **243**, 8–22.

19 L. S. Romsted, in *Supramolecular Chemistry: From Molecules to Nanomaterials*, John Wiley & Sons, Ltd, 2012.

20 I. B. Ivanov, R. I. Slavchov, E. S. Basheva, D. Sidzhakova and S. I. Karakashev, Hofmeister effect on micellization, thin films and emulsion stability, *Adv. Colloid Interface Sci.*, 2011, **168**, 93–104.

21 K. Maiti, D. Mitra, S. Guha and S. P. Moulik, Salt effect on self-aggregation of sodium dodecylsulfate (SDS) and tetradecyltrimethylammonium bromide (TTAB): Physicochemical correlation and assessment in the light of Hofmeister (lyotropic) effect, *J. Mol. Liq.*, 2009, **146**, 44–51.

22 L. Zhang, P. Somasundaran and C. Maltesh, Electrolyte effects on the surface tension and micellization of n-dodecyl β-D-maltoside solutions, *Langmuir*, 1996, **12**, 2371–2373.

23 S. Miyagishi, K. Okada and T. Asakawa, Salt effect on critical micelle concentrations of nonionic surfactants, N-acyl-N-methylglucamides (MEGA-n), *J. Colloid Interface Sci.*, 2001, **238**, 91–95.

24 P. Jungwirth and D. J. Tobias, Molecular structure of salt solutions: A new view of the interface with implications for heterogeneous atmospheric chemistry, *J. Phys. Chem. B*, 2001, **105**, 10468–10472.

25 D. T. Bowron and K. J. Edler, Decyltrimethylammonium Bromide Micelles in Acidic Solutions: Counterion Binding, Water Structuring, and Micelle Shape, *Langmuir*, 2017, **33**, 262–271.

26 W. Wang, W. Sung, M. Ao, N. A. Anderson, D. Vaknin and D. Kim, Halide ions effects on surface excess of long chain ionic liquids water solutions, *J. Phys. Chem. B*, 2013, **117**, 13884–13892.

27 D. Liu, G. Ma, L. M. Levering and H. C. Allen, Vibrational spectroscopy of aqueous sodium halide solutions and air-liquid interfaces: Observation of increased interfacial depth, *J. Phys. Chem. B*, 2004, **108**, 2252–2260.

28 L. Vrbka, M. Mucha, B. Minofar, P. Jungwirth, E. C. Brown and D. J. Tobias, Propensity of soft ions for the air/water interface, *Curr. Opin. Colloid Interface Sci.*, 2004, **9**, 67–73.

29 K. D. Collins, The behavior of ions in water is controlled by their water affinity, *Q. Rev. Biophys.*, 2019, **52**, e11.

30 N. Vlachy, B. Jagoda-Cwiklik, R. Vácha, D. Touraud, P. Jungwirth and W. Kunz, Hofmeister series and specific interactions of charged headgroups with aqueous ions, *Adv. Colloid Interface Sci.*, 2009, **146**, 42–47.

31 H. I. Okur, J. Hladílková, K. B. Rembert, Y. Cho, J. Heyda, J. Dzubiella, P. S. Cremer and P. Jungwirth, Beyond the Hofmeister Series: Ion-Specific Effects on Proteins and Their Biological Functions, *J. Phys. Chem. B*, 2017, **121**, 1997–2014.

32 P. Jungwirth and P. S. Cremer, Beyond hofmeister, *Nat. Chem.*, 2014, **6**, 261–263.

33 J. Song, T. H. Kang, M. W. Kim and S. Han, Ion specific effects: decoupling ion-ion

and ion-water interactions, *Phys. Chem. Chem. Phys.*, 2015, **17**, 8306–8322.

34 A. Salis and B. W. Ninham, Models and mechanisms of Hofmeister effects in electrolyte solutions, and colloid and protein systems revisited, *Chem. Soc. Rev.*, 2014, **43**, 7358–7377.

35 K. D. Collins, Why continuum electrostatics theories cannot explain biological structure , polyelectrolytes or ionic strength effects in ion – protein interactions, *Biophys. Chem.*, 2012, **167**, 43–59.

36 R. Haen, *HYDRANAL manual*, Fifth edit., 1988.

37 Christensen, J.J., Eatough, D.J., Izatt, R.M., *Handbook of Metal Ligand Heats and Related Thermodynamic Quantities*, Marcel Dekker, Inc., New York, 1975.

38 N. Patsos, K. Lewis, F. Picchioni and M. N. Kobrak, Extraction of acids and bases from aqueous phase to a pseudoprotic ionic liquid, *Molecules*, 2019, **24**, 894.

39 A. H. Narten, A. Habenschuss, K. G. Honnell, J. D. McCoy, J. G. Curro and K. S. Schweizer, Diffraction by macromolecular fluids, *J. Chem. Soc. Faraday Trans.*, 1992, **88**, 1791–1795.

40 K. Monar and A. Habenschuss, Modeling the principal amorphous halo in quiescent melts of polyethylene and ethylene copolymers using wide-angle X-ray scattering and its implications, *J. Polym. Sci. Part B Polym. Phys.*, 1999, **37**, 3401–3410.

41 U. Salma, P. Ballirano, M. Usula, R. Caminiti, N. V. Plechkova, K. R. Seddon and L. Gontrani, A new insight into the nanostructure of alkylammonium alkanoates based ionic liquids in water, *Phys. Chem. Chem. Phys.*, 2016, **18**, 11497.

42 X. Gao, R. Tian, X. Liu, H. Zhu, Y. Tang, C. Xu, G. M. Shah and H. Li, Specific ion effects of Cu2+, Ca2+ and Mg2+ on montmorillonite aggregation, *Appl. Clay Sci.*, 2019, DOI:10.1016/j.clay.2019.105154.

43 J. Hu, Q. Chen, H. Hu, Z. Jiang, D. Wang, S. Wang and Y. Li, Microscopic insights into extraction mechanism of copper(II) in ammoniacal solutions studied by X-ray absorption spectroscopy and density functional theory calculation., *J. Phys. Chem. A*, 2013, **117**, 12280–7.

44 F. M. Al-Sogair, B. P. Operschall, A. Sigel, H. Sigel, J. Schnabl and R. K. O. Sigel, Probing the metal-ion-binding strength of the hydroxyl group, *Chem. Rev.*, 2011, **111**, 4964–5003.

45 H. Ghanadzadeh and S. Abbasnejad, Separation of Copper (II) with Solvent Extraction Using Lauric acid Diluted in Benzene, *J. Thermodyn. Catal.*, 2011, **02**, 2–7.

46 D. Suhendra, K. P. Yeen, M. J. Haron, S. Silong, M. Basri and W. M. Z. W. Yunus, Copper ion extraction by a mixture of fatty hydroxamic acids synthesized from commercial palm olein, *Solvent Extr. Ion Exch.*, 2005, **23**, 713–723.

ASSOCIATED CONTENT

The supporting information provides the following contents:

- Additional information about the experimental work.
- The graphs of the SAXS results for the trioctylamine/decanoic acid mixtures as well for the trioctylamine/oleic acid mixtures.
- Details about the analysis for low-q values for the A31 $Cu(NO_3)_2$ and $CuCl_2$ experiments.
- Fitting results for the A31 organic phase of A31-$Cu(NO_3)_2$ (top) and A31-$CuCl_2$ (bottom)extraction experiments
- Details about the determination of peak widths

AUTHOR INFORMATION

Corresponding Author

* Dr. Camiel H.C. Janssen*
Departamento de Ingeniería Química
Facultad de Química
Universidad Nacional Autónoma de México
Circuito exterior S/N, Coyoacán, Ciudad de México
Email: engineerjanssen@gmail.com

Author Contributions

The manuscript was written through contributions of all authors. All authors have given approval to the final version of the manuscript.